

TABLE 1

Star	W(A)	[O/H]	[Fe/H]		[Ca/H]
HD 2857	0.41	-0.4	-1.3	-1.9	
HD 74721	0.61	+0.1		-1.2	0.0
HD 86986	0.57	0.0		-1.6	-2.0
HD 117880	0.58	0.0			-1.0
HD 130095	0.32	-0.7	-0.6		-0.6
HD 139961	0.53	-0.1			-1.6
HD 213468	0.43	-0.3			<-1.1

Values of [Fe/H] are (from left to right) from Kodaira and Davis Philip (1981), Danfort and Lea (1981), Klochkova and Panchuk (1985). [Ca/H] values are from Rodgers (1972).

normalized to the continuum level, are shown in the second column of Table 1 for all the programme field HB stars. Their accuracy should be of the order of 15%, the main source of error being the continuum position. A comparison with previous observations may be done only for HD 86986, whose OI triplet equivalent width was found $0.65 \pm 0.13 \text{ \AA}$ by Kodaira and Tanaka from an image-tube spectrum. Given the observational errors, the agreement may be considered good.

As it was told above, the formation of this OI absorption triplet happens in strong non-LTE conditions, which have been extensively studied by Baschek, Scholz and Sedlmayr (1977). From their computations it is clear that temperature and gravity differences have only a small effect on the total equivalent width of the triplet for HB A-type stars, while major effects are expected from microturbulence and metal content variations. Several determinations of Te and log(g)

are available for the present stars (see Huenemoerder, de Boer and Code 1984 for the most recent results) all in fair agreement among them. On the contrary, microturbulence has been measured for only 4 stars, and there is no agreement between different authors. However, the spread of this parameter is not large when stars observed with the same instrument are compared, and the resulting maximum spread in the triplet equivalent widths should be less than 20%. If one assumes, as a first approximation, that microturbulence is nearly the same for all the programme stars, then the ranking in oxygen equivalent width may be considered as a ranking in abundance too.

From the paper of Baschek et al. one may roughly derive that $\Delta \log [O/H] \sim 2.8 \Delta \log (W_\lambda)$ for $[O/H] \sim -1$ and a microturbulence of 5 km/s. This allows a preliminary conversion from equivalent widths to relative abundances to be made, which is shown in column 3 of

Table 1, where HD 86986 is taken as reference star. The definition of the trend of [O/H] vs [Fe/H] is not possible by now, because a homogeneous set of [Fe/H] determinations is not available and the published values, also collected in Table 1, are clearly inadequate. A first result that can be remarked, however, is that the oxygen abundances found span a range of about a factor 6 within this star sample, with the most oxygen-poor star being relatively iron rich. It may also be noted that the [Ca/H] ranking found by Rodgers (1972) from the H and K line intensities in low dispersion spectra does not agree with the present (preliminary) [O/H] ranking. A homogeneous set of spectroscopic (blue) observations of these stars is clearly needed to derive their microturbulence and [Fe/H] values and then the trend of [O/Fe].

References

- Baschek, B., Scholz, M., Sedlmayr, E., 1977, *Astron. Astrophys.* **55**, 375.
 Butler, D., Laird, J.B., Eriksson, K., Manduca, A., 1986, *Astron. J.* **91**, 570.
 Danfort, S.C., Lea, S.M., 1981, *Astron. J.* **86**, 1909.
 Huenemoerder, D.P., de Boer, K.S., Code, A.D., 1984, *Astron. J.* **89**, 851.
 Klochkova, V.G., Panchuk, V.E., 1985, *Sov. Astron.* **29**, 320.
 Kodaira, K., Tanaka, K., 1972, *Publ. Astron. Soc. Japan* **24**, 355.
 Kodaira, K., Davis Philip, A.G., 1981, IAU Coll. No. 68, 153.
 Peterson, R.C., 1985, *Astrophys. J.* **289**, 320.
 Pilachowsky, C.A., Sneden, C., Wallerstein, G., 1983, *Astrophys. J. Suppl.* **52**, 241.
 Rodgers, A.W., 1972, *Mon. Not. R. Astron. Soc.* **146**, 71.

The Optical Counterpart of OH/IR 17.7-2.0

T. LE BERTRE, ESO

Type-II OH sources are characterized by maser emission at 1,612 MHz (18 cm), with a double-peaked velocity pattern. The emission is supposed to arise in an expanding circumstellar shell, the blue-shifted peak being produced in its front side, and the red-shifted peak in its back side. In such a model, the velocity separation is equal to twice the expansion velocity of the circumstellar envelope. Very often, these sources are associated with long-period variables of spectral type later than M5, such as Miras or supergiants whose spectral energy distributions peak at $\sim 2 \mu\text{m}$. Systematic radio surveys have led to the discovery of numerous type-II OH masers not associated to previously known stellar objects. Research of counter-

parts at infrared wavelengths have led to the discovery of objects extremely red to the point that they could not be identified optically. For that reason, these new objects have been designated "unidentified OH/IR sources". As they show similarities, in the OH and IR properties, with Miras or supergiants, they have been considered to be cool stars in the late stages of evolution on the Ascending Giant Branch (AGB), or core-helium burning supergiants (de Jong, 1983). These stars are in a phase of enhanced mass loss and, consequently, produce an envelope so dense that they are completely hidden to observers at short wavelengths; this phase is assumed to precede the planetary nebula stage. Usually, the energy dis-

tribution is dominated by reradiation from circumstellar dust grains and, except for a feature at $10 \mu\text{m}$, it is similar to that of a blackbody at a temperature lower than $\sim 1,000 \text{ K}$. The $10 \mu\text{m}$ feature is generally attributed to silicate grains and characterizes oxygen-rich circumstellar matter. The prototype of this class of objects is OH/IR 26.5+0.6: its spectrum, comparable to the one of a blackbody at $\sim 400 \text{ K}$, peaks around $10 \mu\text{m}$ and it is not detected at $\lambda < 2 \mu\text{m}$. It is variable in the IR and OH emissions, with a very long period ($P \sim 1,630 \text{ days}$). From the OH spectrum, the expansion velocity is $\sim 14 \text{ km s}^{-1}$. Using the Very Large Array (VLA), Herman et al. (1985) resolved the OH-shell structure and showed it to be

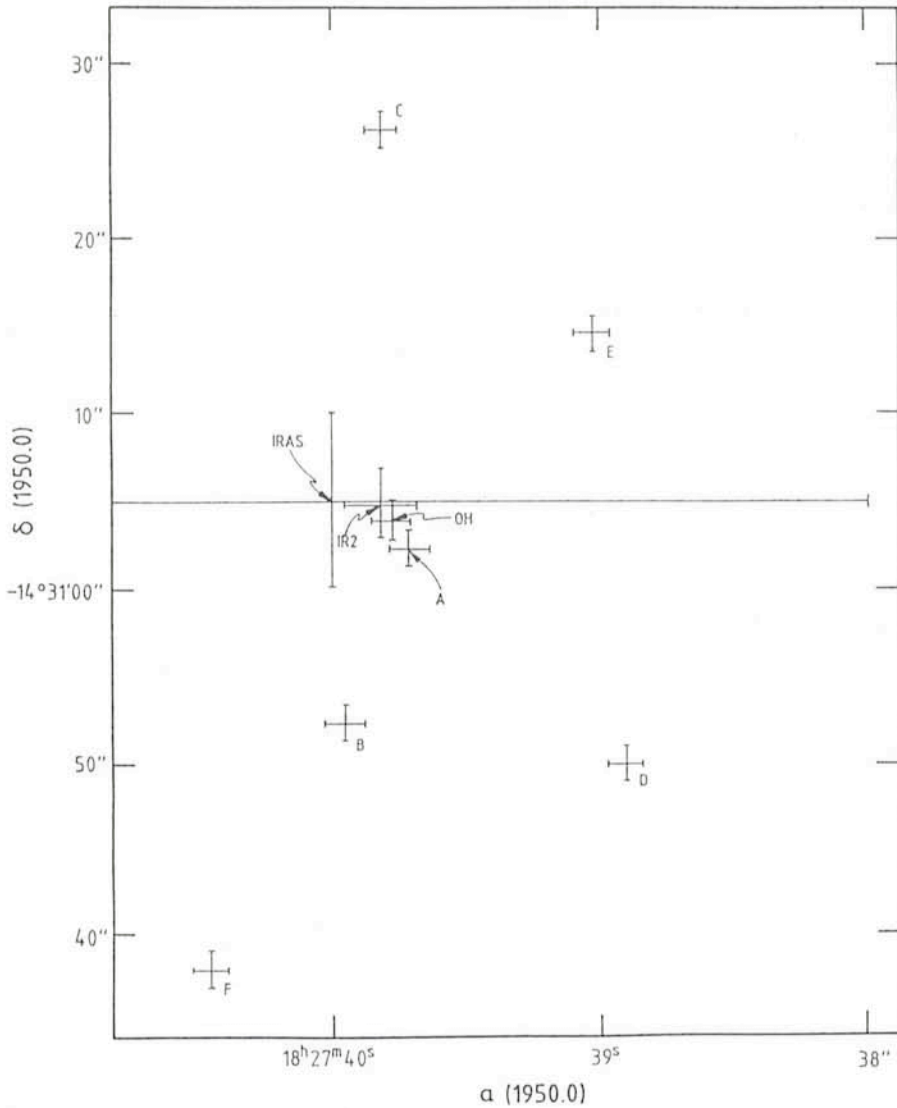


Figure 1: Positions of OH/IR 17.7–2.0, measured in different wavelength ranges (IRAS [10–100 μm]; IR2 [2 μm]; OH [18 cm]; A [0.5 μm]). Positions of some field objects (B, C, D, E, F) are also indicated.

spherical with a radius of 2.2"; measuring the phase delay between the blue and the red peaks of OH emission, they deduce a distance of 1 kpc. At this distance, the luminosity is $\sim 18 \times 10^3 L_{\odot}$, and the mass-loss rate, $5 \times 10^{-5} M_{\odot} \text{ yr}^{-1}$.

Another famous unidentified OH/IR source is OH/IR 17.7–2.0. It has a typical type-II OH spectrum, indicative of an average expansion velocity ($V_e \sim 14 \text{ km s}^{-1}$). As its energy distribution is peaking at 30 μm , there should be no hope to find any optical counterpart. Nevertheless, in some aspects this object appears to be peculiar. Bowers et al. (1981), using also the VLA, showed that the structure is not spherical, but elongated ($3.1 \times 1.4''$). Norris et al. (1984) discovered in the OH spectrum a high-velocity feature (600 km s^{-1}) which might indicate that a violent phenomenon is occurring in this source. Finally, Sèvre (1984) discovered what could be an optical counterpart of OH/IR 17.7–2.0.

As stated above, such an identification was absolutely unexpected and,

consequently, deserved careful attention. As this source is in a region near the galactic plane, which is very crowded, there was a high probability of confusion. Also, it could be possible that a background star was exactly coincident with the real OH/IR source. Clearly, the first step was to select or obtain the best possible coordinates in different wavelength ranges.

Bowers et al. (1981), with the VLA, measured a radio position (labelled OH on Figure 1) which is accurate to $\pm 1''$. In the visible, by using the Optronics machine of ESO-Garching, it is possible to measure positions on Schmidt plates with an accuracy of $\pm 1''$; this has been done for the objects in the field of the OH position (labels: A, B, C, D, E, F). At this level of investigation, it appears that the Sèvres' object (A) is the only possible counterpart of the OH source, visible on the Sky Atlas plates. The near infrared position of the OH/IR source could be measured, using the 1-m telescope on La Silla. With this telescope, in the pointing mode, by referring to Perth 70 astrometric stars, it is possible to measure absolute positions to within $\sim 7''$. Using it in the offset mode, it is possible to obtain relative positions accurate to $\sim 2''$. By doing so, and using a nearby star whose coordinates were measured with the Optronics machine, the position of the IR source was obtained, at 2 μm , with an accuracy of $\sim 3''$ (label IR2). Once again, the only possible optical counterpart is object A. The IRAS satellite measured a position in the (10–100 μm) range which is labelled IRAS on Figure 1. Due to the field of view of the detectors and to the scanning mode of observation, the error box is wide and elongated; nevertheless, it is interesting to note that all the three posi-

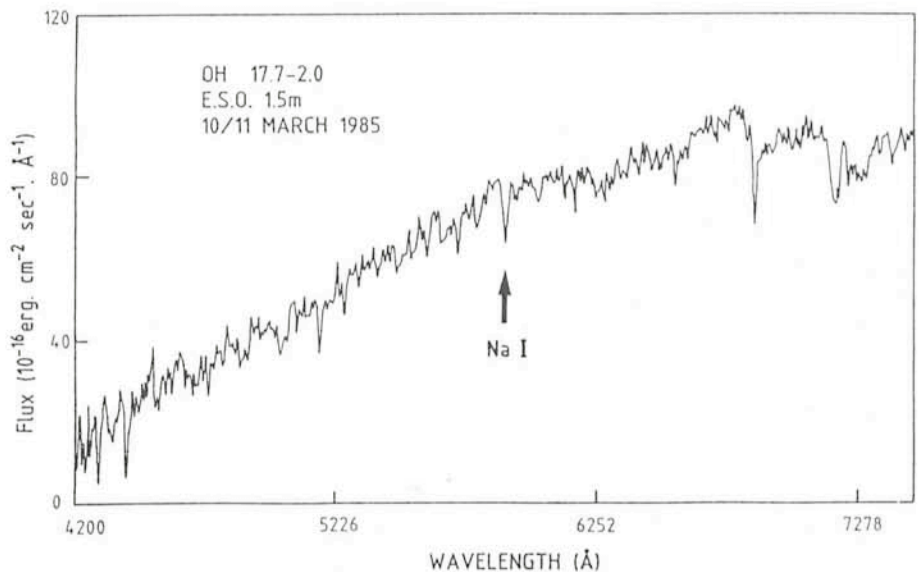


Figure 2: (4200–7500 \AA) IDS spectrum of the optical counterpart of OH/IR 17.7–2.0. The spectral resolution is $\sim 15 \text{ \AA}$; the calibration in fluxes is accurate to $\sim 30\%$.

tions, obtained in very different wavelength ranges and with different instruments, are consistent with A.

This positional agreement does not imply a physical association between A and OH/IR 17.7–2.0. On March 10/11 1985, a spectrum of A was obtained with the Bollers & Chivens spectrograph attached to the 1.5-m telescope and equipped with an IDS detector. This spectrum is presented in Figure 2; the resolution (FWHM) is $\sim 15 \text{ \AA}$. Whereas one would have expected a spectrum dominated by molecular bands, such as those due to TiO and, eventually, VO, like in Mira or M supergiants, at first glance, it looks desperately flat. A few absorption features, like the NaI doublet at 5893 \AA , are visible and point towards an early K-type object. Could it be that the object A is a star, merely coincident with the OH/IR source?

To elucidate this problem, the 1-m telescope was again used, but, this time, for obtaining the broad band energy distribution between $.4$ and $20 \mu\text{m}$. This telescope may be equipped with two photometers, one for the visual range, and one for the infrared. In June 1985, (U, B, V, R, I) data were obtained with the visible photometer and a Quantacon photomultiplier; as the field is very crowded, the sky was measured at positions predetermined with the Optonics on Schmidt plates. The IR photometer equipped with an InSb detector was used to measure the source in the (J, H, K, L, M) bands; similarly, care was taken for avoiding pollution from the chopped beams. Fluxes at 10 and $20 \mu\text{m}$ were measured with a bolometer detector. All these data are plotted in Figure 3, together with those obtained by the IRAS satellite during 1983. The whole spectrum is characterized by a continuity in the variations of the fluxes, indicating that no misidentification has been made. From the (N1, N2, N3) measurements one suspects the presence of the $10 \mu\text{m}$ silicate feature in absorption. It is difficult to explain quantitatively this kind of spectrum by the addition of spectra produced by two different objects, such as the one of a typical OH/IR source peaking at $30 \mu\text{m}$, and the one of a K star; from (U, B, V, R, I) data, a K background star could not be very much reddened, and, with such a modelling, a deficit of energy appears in the $1\text{--}5 \mu\text{m}$ range. In fact, this kind of spectrum seems to be typical of stars embedded in an axi-symmetrical dust shell; for instance, the bipolar nebula CRL 2688 has a very similar broad band energy distribution (Ney et al., 1975).

The observations with the 1-m telescope point towards a physical association between the IR source and object A. This interpretation could be strength-

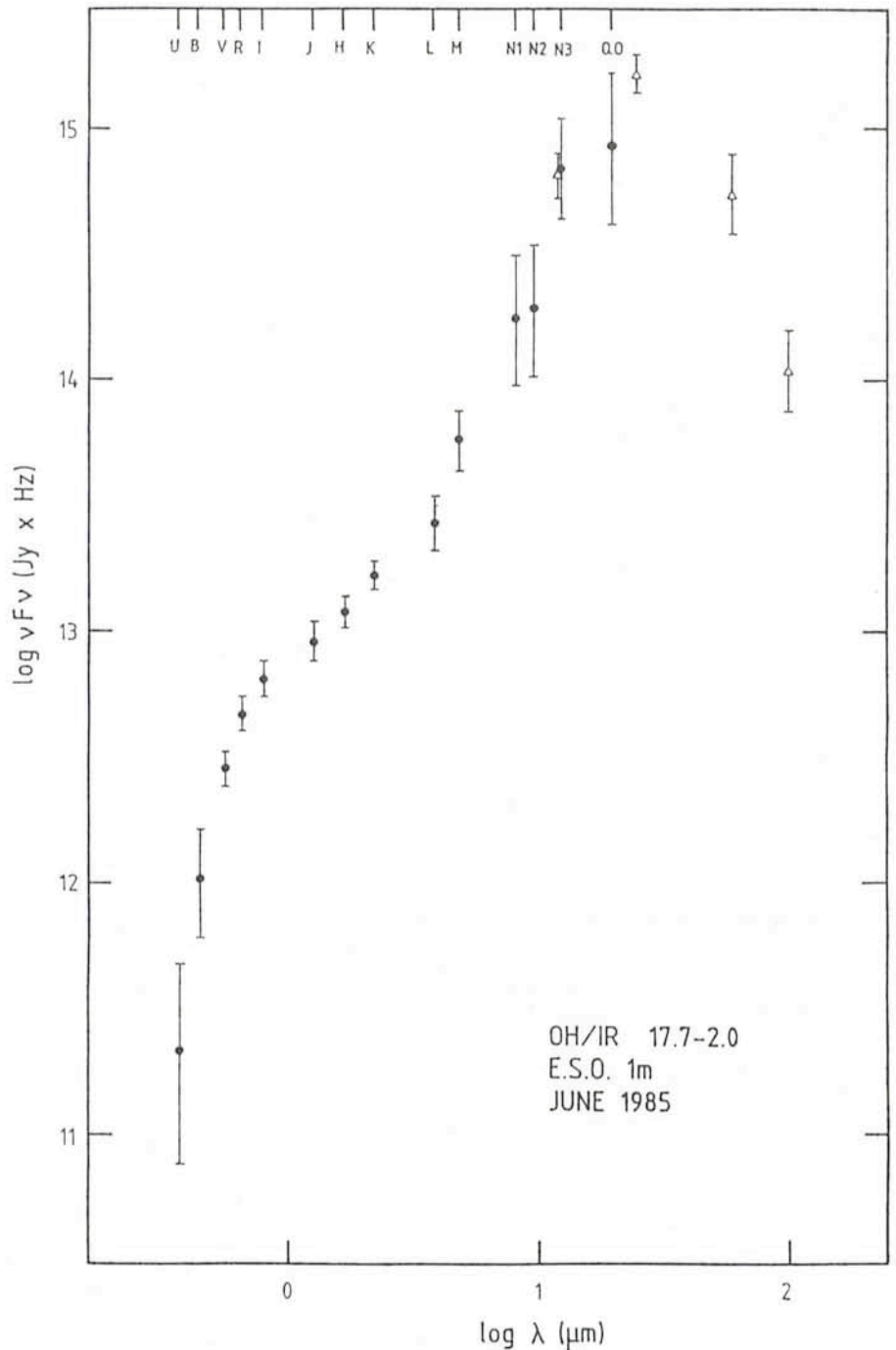


Figure 3: Broad band energy distribution of OH/IR 17.7–2.0. The filled circles (●) correspond to data obtained with the 1-m telescope; the triangles (Δ), to IRAS data.

ened by a confirmation of the central star spectral type independent of optical observations of A. Low resolution spectra can be recorded in the infrared by using the standard ESO photometers; Circular Variable Filters (CVF) are included in those and give a spectral resolution of ~ 60 . M stars are characterized in the $1\text{--}5 \mu\text{m}$ region by the presence of molecular absorption features, mainly due to CO and H_2O . As the object is relatively faint, it was necessary to observe it with the 3.6-m telescope. The recorded spectrum is presented in Figure 4. Once again, the surprising character is the absence of

absorption features, in particular, the usually strong absorption band due to CO at $2.3 \mu\text{m}$ is obviously not present. This absence indicates that the underlying star is of spectral type earlier than K5 and, consequently, is a confirmation of the physical association between OH/IR 17.7–2.0 and A.

OH/IR 17.7–2.0 appears now to be not so "unidentified" as previously thought. The CVF and IDS spectra indicate that it is in a more evolved stage than the one of AGB or M supergiant stars. Objects like OH/IR 17.7–2.0, while they are still type-II OH emitters, could be already evolving towards the

planetary stage, through an axisymmetrical structure reminiscent of bipolar nebulae. Further observations exploiting this still unique opportunity of studying the central star of a type-II OH/IR source are in progress; and, of course, other optical counterparts are actively searched for.

References

- Bowers, P.F., Johnston, K.J., and Spencer, J.H.: 1981, *Nature* **291**, 382.
 Herman, J., Baud, B., Habing, H.J., and Winnberg, A.: 1985, *Astron. Astrophys.* **143**, 122.
 de Jong, T.: 1983, *Astrophys. J.* **274**, 252.
 Ney, E.P., Merrill, K.M., Becklin, E.E., Neugebauer, G., and Wynn-Williams, C.G.: 1975, *Astrophys. J. Letters* **198**, L129.
 Norris, R.P., Booth, R.S., Diamond, P.J., Graham, D.A., and Nyman, L.-A.: 1984, *IAU Symposium* 110, 323.
 Sèvre, F.: 1984, Personal communication.

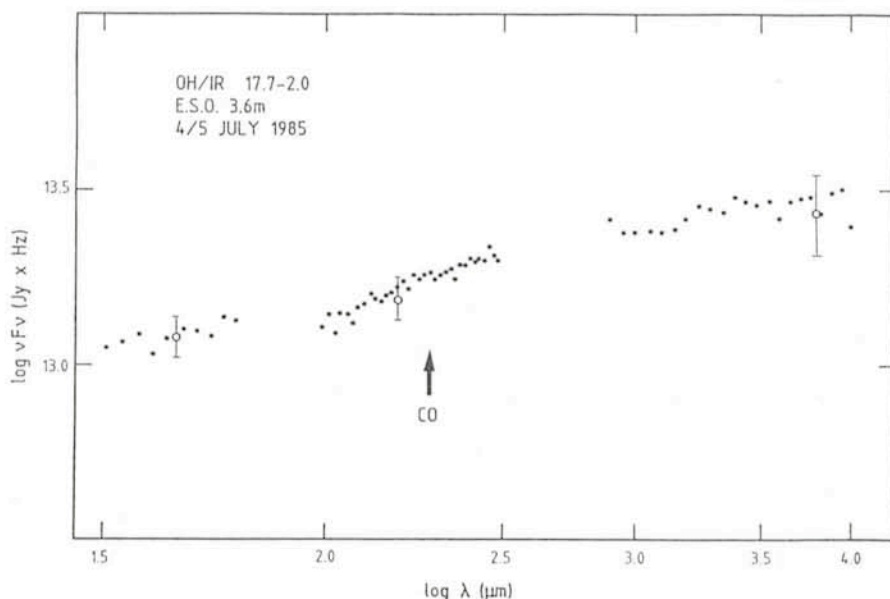


Figure 4: (1.5–4 μm) CVF spectrum of OH/IR 17.7–2.0. The empty circles (o) correspond to the broad band (H, K, L) data obtained at the 1-m telescope (same as in Figure 3). The arrow indicates the position of the 2.3 μm absorption band produced by CO, and, normally, found in M stars.

Infrared Observations of Comet Halley Near Perihelion

T. LE BERTRE, P. BOUCHET and A. CHALABAEV, ESO

A. C. DANKS, Michigan State University

T. ENCRENAZ and N. EPCHEIN, Observatoire de Paris-Meudon

Ground-based observations of periodic Comet Halley near its perihelion passage were important due to the increased activity of its nucleus as it approached the sun and, in this specific case, due to the planned spacecraft flybys several weeks later. As with all comets, it naturally reached its maximum brightness at perihelion, but, of course, it was then so close to the sun that it was difficult to see or measure. It is the cometary astronomers' misfortune that the best moments to catch a comet at its brightest are just before sunrise, or just after sunset. Few ESO telescopes can be used to observe the comet so close to the sun. Among them, the GPO which can almost be pointed to the horizon, and the 1-m telescope which, when equipped for IR observations, can be used for daytime observing. Our principal interest was to monitor the comet progress and evolution in the IR using both the ESO 3.6-m and 1-m telescopes. As a single group, we had sufficient time spaced around perihelion to monitor the comet fairly well. In addition, we were able to fill some of the remaining holes with the kind cooperation of 1-m observers B. Reipurth, H. Cuyper and G. Hahn, who allowed us to observe

1 or 2 hours each day during their observing runs.

During this time, between December 24, 1985, and March 3, 1986, the 1-m telescope was used for approximately three periods of two weeks each. The orbit of the comet brought it from the northern hemisphere to the southern hemisphere, steadily brightening, and, from February 17 to March 3, the comet was undoubtedly well located ($\delta \sim -14^\circ$) for observations from La Sila. The comet was west of the sun in this period and, consequently, observable in the morning; due to the configuration of the Andes the sunrise was delayed by approximately 15 minutes. These 15 minutes or so were crucial in the period from February 17 to 18 when the comet was at less than 20° from the sun. The 1-m telescope was equipped with an InSb detector for the 1 to 5 μm range or a bolometer for the 8 to 20 μm range. Both instruments employ a focal plane chopper, and chopping was carried out in the east-west direction with a 30 arc-seconds amplitude. This naturally means, due to the large angular size of the comet, that with one beam centred on the nucleus, the other beam was somewhere in the coma.

In Figure 1, the broad band flux distribution is shown plotted against wavelength. Although the dust grains expelled from the nucleus constitute, in mass, only a minor fraction of the material, they are the dominant element responsible for the observed broad-band IR spectrum. The flux distribution can be seen to consist of two different regimes: from 1 to $\sim 3 \mu\text{m}$, the spectrum is dominated by dust-scattered sunlight, whereas at wavelengths longer than 3 μm , thermal emission from the dust is dominating, and described well by a 400°K blackbody (no wavelength dependence of emissivity has been taken into account). The spectrum is qualitatively similar to that found in comets Bennett, Kohoutek and Bradfield (see e.g., Ney, E.P.: 1974, *Icarus* **23**, 551).

In Figure 2, the evolution of individual bands and colours is shown with time, over the period between February 17 and March 3, 1986. One measurement a day was made at approximately 10 hours UT, and the observations were, therefore, carried out during day time, centring the comet by maximizing the detector signal. This procedure worked well as there was found to be no wavelength dependence with this